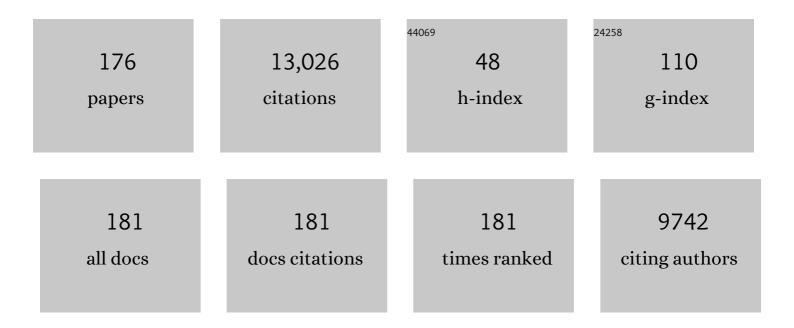
List of Publications by Year in descending order

Source: https://exaly.com/author-pdf/3807055/publications.pdf Version: 2024-02-01



Ηλιμινιίαο

#	Article	IF	CITATIONS
1	Dissociative adsorption of H2O and CO2 on the clean and O-pre-covered high index Ru surfaces: Corrugated Ru(11â^21) and stepped Ru(20â^21) surfaces. Surface Science, 2022, 715, 121936.	1.9	3
2	Catalytic and mechanistic studies of a highly active and <i>E</i> -selective Co( <scp>ii</scp> ) PNN <sup>H</sup> pincer catalyst system for transfer-semihydrogenation of internal alkynes. Inorganic Chemistry Frontiers, 2022, 9, 761-770.	6.0	5
3	( <i>In situ</i> ) spectroscopic studies on state-of-the-art Pd( <scp>ii</scp> ) catalysts in solution for the alkoxycarbonylation of alkenes. Catalysis Science and Technology, 2022, 12, 3175-3189.	4.1	5
4	Unraveling the Synergetic Effect of the FeO <sub><i>x</i></sub> –Cu Model System in Catalyzing the Water–Gas Shift Reaction. Journal of Physical Chemistry C, 2022, 126, 6241-6248.	3.1	1
5	Regiodivergent Reductive Opening of Epoxides by Catalytic Hydrogenation Promoted by a (Cyclopentadienone)iron Complex. ACS Catalysis, 2022, 12, 235-246.	11.2	17
6	Surface hydroxyl dependent adsorption of ruthenium on SiO2(0 0 1) – Understanding metal–support interaction. Applied Surface Science, 2022, 593, 153396.	6.1	3
7	Revisiting Oxygen Adsorption on Ir(100). Journal of Physical Chemistry C, 2022, 126, 10035-10044.	3.1	7
8	Mechanisms of CO2 hydrogenative conversion on supported Ni/ZrO2 catalyst. Applied Surface Science, 2022, 600, 154151.	6.1	3
9	Interactive network of the dehydrogenation of alkanes, alkenes and alkynes – surface carbon hydrogenative coupling on Ru(111). Catalysis Science and Technology, 2021, 11, 191-210.	4.1	4
10	A General and Highly Selective Palladium atalyzed Hydroamidation of 1,3â€Diynes. Angewandte Chemie, 2021, 133, 375-383.	2.0	7
11	A General and Highly Selective Palladium atalyzed Hydroamidation of 1,3â€Diynes. Angewandte Chemie - International Edition, 2021, 60, 371-379.	13.8	26
12	Dehydropolymerisation of methylamine borane using highly active rhodium( <scp>iii</scp> ) bis(thiophosphinite) pincer complexes: catalytic and mechanistic insights. Catalysis Science and Technology, 2021, 11, 3514-3526.	4.1	8
13	Efficient Palladiumâ€Catalyzed Carbonylation of 1,3â€Dienes: Selective Synthesis of Adipates and Other Aliphatic Diesters. Angewandte Chemie - International Edition, 2021, 60, 9527-9533.	13.8	26
14	Efficient Palladiumâ€Catalyzed Carbonylation of 1,3â€Dienes: Selective Synthesis of Adipates and Other Aliphatic Diesters. Angewandte Chemie, 2021, 133, 9613-9619.	2.0	4
15	Nonoxidative Conversion of Methane, Ethane, and Ethylene on Flat Ir(111) and Stepped Ir(211) Surfaces. Journal of Physical Chemistry C, 2021, 125, 5602-5615.	3.1	1
16	Catalytic Activity of Aliphatic PNP Ligated Co <sup>III/I</sup> Amine and Amido Complexes in Hydrogenation Reaction—Structure, Stability, and Substrate Dependence. ACS Catalysis, 2021, 11, 4593-4605.	11.2	6
17	Pyrimidopteridine-Catalyzed Hydroamination of Stilbenes with Primary Amines: A Dual Photoredox and Hydrogen Atom Transfer Catalyst. ACS Catalysis, 2021, 11, 4862-4869.	11.2	15
18	Adsorption of CO, H2, H2O, and CO2 on Fe-, Co-, Ni-, Cu-, Pd-, and Pt-Doped Mo2C(101) Surfaces. Journal of Physical Chemistry C, 2021, 125, 11419-11431.	3.1	3

#	Article	IF	CITATIONS
19	Mechanisms of Co <sup>II</sup> and Acid Jointly Catalyzed Domino Conversion of CO <sub>2</sub> , H <sub>2</sub> , and CH <sub>3</sub> OH to Dialkoxymethane: A DFT Study. ACS Catalysis, 2021, 11, 6908-6919.	11.2	9
20	The Facile Dissociation of Carbon–Oxygen Bonds in CO <sub>2</sub> and CO on the Surface of LaCoSiH <sub><i>x</i></sub> Intermetallic Compound. Angewandte Chemie - International Edition, 2021, 60, 25538-25545.	13.8	17
21	The Facile Dissociation of Carbon–Oxygen Bonds in CO <sub>2</sub> and CO on the Surface of LaCoSiH <sub><i>x</i></sub> Intermetallic Compound. Angewandte Chemie, 2021, 133, 25742-25749.	2.0	0
22	Zirconium-hydride-catalyzed site-selective hydroboration of amides for the synthesis of amines: Mechanism, scope, and application. Chinese Journal of Catalysis, 2021, 42, 2059-2067.	14.0	13
23	Cycloaddition mechanisms of CO <sub>2</sub> and epoxide catalyzed by salophen – an organocatalyst free from metals and halides. Catalysis Science and Technology, 2021, 11, 2529-2539.	4.1	8
24	Synthesis of Phosphinines from Co <sup>II</sup> -Catalyzed [2+2+2] Cycloaddition Reactions. ACS Catalysis, 2021, 11, 13434-13444.	11.2	10
25	A recyclable CoGa intermetallic compound catalyst for the hydroformylation reaction. Journal of Catalysis, 2021, 404, 244-249.	6.2	11
26	Simple mechanisms of CH <sub>4</sub> reforming with CO <sub>2</sub> and H <sub>2</sub> O on a supported Ni/ZrO <sub>2</sub> catalyst. Physical Chemistry Chemical Physics, 2021, 23, 26392-26400.	2.8	4
27	In situ formation of ZnOx species for efficient propane dehydrogenation. Nature, 2021, 599, 234-238.	27.8	133
28	Hydrogen Adsorption on Ir(111), Ir(100) and Ir(110)—Surface and Coverage Dependence. Surface Science, 2020, 692, 121514.	1.9	8
29	Unraveling the Origins of the Synergy Effect between ZrO <sub>2</sub> and CrO <i><sub>x</sub></i> in Supported CrZrO <i><sub>x</sub></i> for Propene Formation in Nonoxidative Propane Dehydrogenation. ACS Catalysis, 2020, 10, 1575-1590.	11.2	46
30	Mechanistic Aspects of CO Activation and C–C Bond Formation on the Fe/C- and Fe-Terminated Fe <sub>3</sub> C(010) Surfaces. ACS Catalysis, 2020, 10, 877-890.	11.2	21
31	Versatile Fluorinated Building Blocks by Stereoselective (Per)fluoroalkenylation of Ketones. European Journal of Organic Chemistry, 2020, 2020, 70-81.	2.4	8
32	CpCo( <scp>i</scp> ) precatalysts for [2 + 2 + 2] cycloaddition reactions: synthesis and reactivity. Catalysis Science and Technology, 2020, 10, 8005-8014.	4.1	6
33	Hydrocracking of Fused Aromatic Hydrocarbons Catalyzed by Al-Substituted HZSM-5—A Case Study of 9,10-Dihydroanthracene. ACS Catalysis, 2020, 10, 9215-9226.	11.2	13
34	Coverage-Dependent Water Dissociative Adsorption Properties on Nickel Surfaces. Journal of Physical Chemistry C, 2020, 124, 25835-25845.	3.1	6
35	Tuning the Selectivity of Palladium Catalysts for Hydroformylation and Semihydrogenation of Alkynes: Experimental and Mechanistic Studies. ACS Catalysis, 2020, 10, 12167-12181.	11.2	31
36	Structure–Activity–Selectivity Relationships in Propane Dehydrogenation over Rh/ZrO <sub>2</sub> Catalysts. ACS Catalysis, 2020, 10, 6377-6388.	11.2	47

#	Article	IF	CITATIONS
37	Exploring direct and hydrogen-assisted CO activation on iridium surfaces – surface dependent activity. Catalysis Science and Technology, 2020, 10, 4424-4435.	4.1	2
38	Reduction Over Condensation of Carbonyl Compounds Through a Transient Hemiaminal Intermediate Using Hydrazine. Journal of Organic Chemistry, 2020, 85, 9213-9218.	3.2	2
39	Mechanistic Insights into the Chemoâ€Selective Dehydrogenative Silylation of Alkenes Catalyzed by Bis(imino)pyridine Cobalt Complex from DFT Computations. ChemCatChem, 2020, 12, 3890-3899.	3.7	2
40	Molybdenum carbide supported metal catalysts (M <sub>n</sub> /Mo <sub>x</sub> C; M = Co, Ni, Cu, Pd,) Tj ETC 3029-3046.	2q0 0 0 rgl 4.1	3T /Overlock 15
41	Zirconiumâ€Catalyzed Atomâ€Economical Synthesis of 1,1â€Diborylalkanes from Terminal and Internal Alkenes. Angewandte Chemie, 2020, 132, 13710-13714.	2.0	7
42	Zirconiumâ€Catalyzed Atomâ€Economical Synthesis of 1,1â€Diborylalkanes from Terminal and Internal Alkenes. Angewandte Chemie - International Edition, 2020, 59, 13608-13612.	13.8	38
43	Chemoselective semihydrogenation of alkynes catalyzed by manganese( <scp>i</scp> )-PNP pincer complexes. Catalysis Science and Technology, 2020, 10, 3994-4001.	4.1	43
44	General and selective synthesis of primary amines using Ni-based homogeneous catalysts. Chemical Science, 2020, 11, 4332-4339.	7.4	29
45	Determining the structures, acidity and adsorption properties of Al substituted HZSM-5. Physical Chemistry Chemical Physics, 2019, 21, 18758-18768.	2.8	18
46	Coverage dependent structure and energy of water dissociative adsorption on clean and O-pre-covered Ni (100) and Ni(110). Catalysis Science and Technology, 2019, 9, 4725-4743.	4.1	8
47	Nitridation of the metallic Mo2C(001) surface from NH3 dissociative adsorption—A DFT study. Surface Science, 2019, 689, 121466.	1.9	12
48	A selective route to aryl-triphosphiranes and their titanocene-induced fragmentation. Chemical Science, 2019, 10, 7859-7867.	7.4	34
49	Fe(II) Hydride Complexes for the Homogeneous Dehydrocoupling of Hydrazine Borane: Catalytic Mechanism via DFT Calculations and Detailed Spectroscopic Characterization. Organometallics, 2019, 38, 2714-2723.	2.3	12
50	Surface Carbon Hydrogenation on Precovered Fe(110) with Spectator-Coverage-Dependent Chain Initiation and Propagation. Journal of Physical Chemistry C, 2019, 123, 25657-25667.	3.1	6
51	Molecular or dissociative adsorption of water on clean and oxygen pre-covered Ni(111) surfaces. Catalysis Science and Technology, 2019, 9, 199-212.	4.1	9
52	Mechanistic insight into CO activation, methanation and C-C bond formation from coverage dependent CO hydrogenation on Fe(110). Surface Science, 2019, 689, 121456.	1.9	10
53	Mechanism of Graphene Formation via Detonation Synthesis: AÂDFTB Nanoreactor Approach. Journal of Chemical Theory and Computation, 2019, 15, 3654-3665.	5.3	25
54	Mechanisms and Activity of 1â€Phenylethanol Dehydrogenation Catalyzed by Bifunctional NHCâ€Ir <sup>III</sup> Complex. European Journal of Organic Chemistry, 2019, 2019, 3929-3936.	2.4	4

#	Article	IF	CITATIONS
55	1-Titanacyclobuta-2,3-diene – an elusive four-membered cyclic allene. Chemical Science, 2019, 10, 5319-5325.	7.4	26
56	Visiting CH4 formation and C1 + C1 couplings to tune CH4 selectivity on Fe surfaces. Journal of Catalysis, 2019, 372, 217-225.	6.2	19
57	Iron–PNPâ€Pincer atalyzed Transfer Dehydrogenation of Secondary Alcohols. ChemSusChem, 2019, 12, 2988-2993.	6.8	14
58	Cobalt atalyzed Aqueous Dehydrogenation of Formic Acid. Chemistry - A European Journal, 2019, 25, 8459-8464.	3.3	54
59	High-Coverage CO Adsorption and Dissociation on Ir(111), Ir(100), and Ir(110) from Computations. Journal of Physical Chemistry C, 2019, 123, 6487-6495.	3.1	12
60	Enantioselective Hydrogenation of Ketones using Different Metal Complexes with a Chiral PNP Pincer Ligand. Advanced Synthesis and Catalysis, 2019, 361, 1913-1920.	4.3	37
61	Morphology and Reactivity Evolution of HCP and FCC Ru Nanoparticles under CO Atmosphere. ACS Catalysis, 2019, 9, 2768-2776.	11.2	36
62	CO Self-Promoting Hydrogenation on CO-Saturated Ru(0001): A New Theoretical Insight into How H <sub>2</sub> Participates in CO Activation. Journal of Physical Chemistry C, 2019, 123, 6508-6515.	3.1	9
63	The effect of phase composition and crystallite size on activity and selectivity of ZrO2 in non-oxidative propane dehydrogenation. Journal of Catalysis, 2019, 371, 313-324.	6.2	74
64	Exploring the mechanism of alkene hydrogenation catalyzed by defined iron complex from DFT computation. Journal of Molecular Modeling, 2019, 25, 61.	1.8	3
65	Manganese PNP-pincer catalyzed isomerization of allylic/homo-allylic alcohols to ketones – activity, selectivity, efficiency. Catalysis Science and Technology, 2019, 9, 6327-6334.	4.1	14
66	Homogeneous cobalt-catalyzed reductive amination for synthesis of functionalized primary amines. Nature Communications, 2019, 10, 5443.	12.8	57
67	Bifunctional aliphatic PNP pincer catalysts for hydrogenation: Mechanisms and scope. Advances in Inorganic Chemistry, 2019, 73, 323-384.	1.0	13
68	Visiting the Limits between a Highly Strained 1â€Zirconacyclobutaâ€2,3â€diene and Chemically Robust Dizirconacyclooctatetraene. Chemistry - A European Journal, 2018, 24, 5667-5674.	3.3	20
69	Cooperative catalytic methoxycarbonylation of alkenes: uncovering the role of palladium complexes with hemilabile ligands. Chemical Science, 2018, 9, 2510-2516.	7.4	94
70	Selective Baseâ€free Transfer Hydrogenation of α,βâ€Unsaturated Carbonyl Compounds using <i>i</i> PrOH or EtOH as Hydrogen Source. Chemistry - A European Journal, 2018, 24, 2725-2734.	3.3	34
71	Exploring the Chemoselective Dehydrogenative Silylation and Hydrogenation of Divinyldisiloxane with Hydrosilane from DFT Computation. European Journal of Organic Chemistry, 2018, 2018, 1993-1999.	2.4	2
72	Exploring the activities of vanadium, niobium, and tantalumÂPNP pincer complexes in the hydrogenation of phenyl-substituted CN, CN, CC, CC, and CO functional groups. Comptes Rendus Chimie, 2018, 21, 303-309.	0.5	8

#	Article	IF	CITATIONS
73	Isomerization of Allylic Alcohols to Ketones Catalyzed by Wellâ€Defined Iron PNP Pincer Catalysts. Chemistry - A European Journal, 2018, 24, 4043-4049.	3.3	38
74	Toward Green Acylation of (Hetero)arenes: Palladium-Catalyzed Carbonylation of Olefins to Ketones. ACS Central Science, 2018, 4, 30-38.	11.3	22
75	Cobalt Pincer Complexes for Catalytic Reduction of Carboxylic Acid Esters. Chemistry - A European Journal, 2018, 24, 1046-1052.	3.3	63
76	Successive Dissociation of CO, CH <sub>4</sub> , C <sub>2</sub> H <sub>6</sub> , and CH <sub>3</sub> CHO on Fe(110): Retrosynthetic Understanding of FTS Mechanism. Journal of Physical Chemistry C, 2018, 122, 28846-28855.	3.1	11
77	Benyzl Alcohol Dehydrogenative Coupling Catalyzed by Defined Mn and Re PNP Pincer Complexes – A Computational Mechanistic Study. European Journal of Inorganic Chemistry, 2018, 2018, 4643-4657.	2.0	16
78	Aerobic Oxidative Homo- and Cross-Coupling of Amines Catalyzed by Phenazine Radical Cations. Journal of Organic Chemistry, 2018, 83, 13481-13490.	3.2	36
79	Control of coordinatively unsaturated Zr sites in ZrO2 for efficient C–H bond activation. Nature Communications, 2018, 9, 3794.	12.8	133
80	Exploring the mechanisms of aqueous methanol dehydrogenation catalyzed by defined PNP Mn and Re pincer complexes under base-free as well as strong base conditions. Catalysis Science and Technology, 2018, 8, 3649-3665.	4.1	32
81	About the Inversion Barriers of Pâ€Chirogenic Triarylâ€Substituted Phosphanes. European Journal of Organic Chemistry, 2018, 2018, 2984-2994.	2.4	16
82	Mechanisms of CO Activation, Surface Oxygen Removal, Surface Carbon Hydrogenation, and C–C Coupling on the Stepped Fe(710) Surface from Computation. Journal of Physical Chemistry C, 2018, 122, 15505-15519.	3.1	12
83	Potassium promotion on CO hydrogenation on the χ-Fe 5 C 2 (111) surface with carbon vacancy. Applied Catalysis A: General, 2017, 534, 22-29.	4.3	16
84	A Stable Manganese Pincer Catalyst for the Selective Dehydrogenation of Methanol. Angewandte Chemie, 2017, 129, 574-577.	2.0	37
85	Redoxâ€Disproportionation of a Decamethyltitanocene(III) Isonitrile Alkynyl Complex. Chemistry - A European Journal, 2017, 23, 7891-7895.	3.3	14
86	Adsorption and dissociation of H 2 O and CO 2 on the clean and O-pre-covered Ru(0001) surface. Applied Catalysis A: General, 2017, 540, 31-36.	4.3	8
87	Hydrogenation of phenyl-substituted Cî€,N, Cî€N,Cî€,C, Cî€C and Cî€O functional groups by Cr, Mo and W PNP pincer complexes – a DFT study. Catalysis Science and Technology, 2017, 7, 2298-2307.	4.1	11
88	A Stable Manganese Pincer Catalyst for the Selective Dehydrogenation of Methanol. Angewandte Chemie - International Edition, 2017, 56, 559-562.	13.8	158
89	Oxidation of the hexagonal Mo <sub>2</sub> C(101) surface by H <sub>2</sub> O dissociative adsorption. Catalysis Science and Technology, 2017, 7, 2789-2797.	4.1	6
90	Reaction of CO, H <sub>2</sub> 0, H <sub>2</sub> and CO <sub>2</sub> on the clean as well as O, OH and H precovered Fe(100) and Fe(111) surfaces. Catalysis Science and Technology, 2017, 7, 427-440.	4.1	22

#	Article	IF	CITATIONS
91	Mechanism of coverage dependent CO adsorption and dissociation on the Mo(100) surface. Physical Chemistry Chemical Physics, 2017, 19, 2186-2192.	2.8	11
92	Titanocene Silylpropyne Complexes: Promising Intermediates en route to a Fourâ€Membered 1â€Metallacyclobutaâ€2,3â€diene?. Chemistry - A European Journal, 2017, 23, 14158-14162.	3.3	9
93	Location, distribution and acidity of Al substitution in ZSM-5 with different Si/Al ratios – a periodic DFT computation. Catalysis Science and Technology, 2017, 7, 5694-5708.	4.1	30
94	Manganese(I) atalyzed Enantioselective Hydrogenation of Ketones Using a Defined Chiral PNP Pincer Ligand. Angewandte Chemie - International Edition, 2017, 56, 11237-11241.	13.8	180
95	Manganese(I) atalyzed Enantioselective Hydrogenation of Ketones Using a Defined Chiral PNP Pincer Ligand. Angewandte Chemie, 2017, 129, 11389-11393.	2.0	64
96	Ligand―and Solventâ€Tuned Chemoselective Carbonylation of Bromoaryl Triflates. Chemistry - A European Journal, 2017, 23, 13369-13378.	3.3	32
97	About copper promotion in CH 4 formation from CO hydrogenation on Fe(100): A density functional theory study. Applied Catalysis A: General, 2017, 530, 83-92.	4.3	16
98	Activation mechanisms of H 2 , O 2 , H 2 O, CO 2 , CO, CH 4 and C 2 H x on metallic Mo 2 C(001) as well as Mo/C terminated Mo 2 C(101) from density functional theory computations. Applied Catalysis A: General, 2016, 524, 223-236.	4.3	39
99	Improved Second Generation Iron Pincer Complexes for Effective Ester Hydrogenation. Advanced Synthesis and Catalysis, 2016, 358, 820-825.	4.3	104
100	A comparative computationally study about the defined m(II) pincer hydrogenation catalysts (m = fe, ru	ı,) Ţj ETQq	0
101	Methane formation mechanism in the initial methanol-to-olefins process catalyzed by SAPO-34. Catalysis Science and Technology, 2016, 6, 5526-5533.	4.1	43
102	Selective Catalytic Hydrogenations of Nitriles, Ketones, and Aldehydes by Well-Defined Manganese Pincer Complexes. Journal of the American Chemical Society, 2016, 138, 8809-8814.	13.7	485
103	Kinetics and thermodynamics of polymethylbenzene formation over zeolites with different pore sizes for understanding the mechanisms of methanol to olefin conversion – a computational study. Catalysis Science and Technology, 2016, 6, 5326-5335.	4.1	21
104	Mechanisms of Mo2C(101)-Catalyzed Furfural Selective Hydrodeoxygenation to 2-Methylfuran from Computation. ACS Catalysis, 2016, 6, 6790-6803.	11.2	51
105	Hydrogenation of Esters to Alcohols Catalyzed by Defined Manganese Pincer Complexes. Angewandte Chemie - International Edition, 2016, 55, 15364-15368.	13.8	259
106	Hydrogenation of Esters to Alcohols Catalyzed by Defined Manganese Pincer Complexes. Angewandte Chemie, 2016, 128, 15590-15594.	2.0	88
107	Mechanisms of H <sub>2</sub> O and CO <sub>2</sub> Formation from Surface Oxygen Reduction on Co(0001). Journal of Physical Chemistry C, 2016, 120, 19265-19270.	3.1	25
108	When Density Functional Approximations Meet Iron Oxides. Journal of Chemical Theory and Computation, 2016, 12, 5132-5144.	5.3	102

#	Article	IF	CITATIONS
109	How far away are iron carbide clusters from the bulk?. Physical Chemistry Chemical Physics, 2016, 18, 32944-32951.	2.8	12
110	Mechanisms of H- and OH-assisted CO activation as well as C–C coupling on the flat Co(0001) surface – revisited. Catalysis Science and Technology, 2016, 6, 8336-8343.	4.1	18
111	Unravelling the Mechanism of Basic Aqueous Methanol Dehydrogenation Catalyzed by Ru–PNP Pincer Complexes. Journal of the American Chemical Society, 2016, 138, 14890-14904.	13.7	155
112	Surface morphology of orthorhombic Mo2C catalyst and high coverage hydrogen adsorption. Surface Science, 2016, 651, 195-202.	1.9	23
113	Stability and Reactivity of Intermediates of Methanol Related Reactions and C–C Bond Formation over H-ZSM-5 Acidic Catalyst: A Computational Analysis. Journal of Physical Chemistry C, 2016, 120, 6075-6087.	3.1	50
114	Theoretical study about Mo <sub>2</sub> C(101)-catalyzed hydrodeoxygenation of butyric acid to butane for biomass conversion. Catalysis Science and Technology, 2016, 6, 4923-4936.	4.1	30
115	Structures of seven molybdenum surfaces and their coverage dependent hydrogen adsorption. Physical Chemistry Chemical Physics, 2016, 18, 6005-6012.	2.8	23
116	Morphology control of K2O promoter on HÃǥg carbide (ï‡-Fe5C2) under Fischer–Tropsch synthesis condition. Catalysis Today, 2016, 261, 93-100.	4.4	35
117	Hydrogenation of Aliphatic and Aromatic Nitriles Using a Defined Ruthenium PNP Pincer Catalyst. European Journal of Organic Chemistry, 2015, 2015, 5944-5948.	2.4	51
118	Coverage dependent water dissociative adsorption on Fe(110) from DFT computation. Physical Chemistry Chemical Physics, 2015, 17, 8811-8821.	2.8	60
119	Exploring Furfural Catalytic Conversion on Cu(111) from Computation. ACS Catalysis, 2015, 5, 4020-4032.	11.2	109
120	Reactions of CO, H <sub>2</sub> O, CO <sub>2</sub> , and H <sub>2</sub> on the Clean and Precovered Fe(110) Surfaces – A DFT Investigation. Journal of Physical Chemistry C, 2015, 119, 28377-28388.	3.1	40
121	Determining surface structure and stability of ε-Fe2C, χ-Fe5C2, Î,-Fe3C and Fe4C phases under carburization environment from combined DFT and atomistic thermodynamic studies. Journal of Lithic Studies, 2015, 1, 44-60.	0.5	50
122	Surface Morphology of Cu Adsorption on Different Terminations of the HÃgg Iron Carbide (χ-Fe <sub>5</sub> C <sub>2</sub> ) Phase. Journal of Physical Chemistry C, 2015, 119, 7371-7385.	3.1	14
123	High coverage adsorption and co-adsorption of CO and H <sub>2</sub> on Ru(0001) from DFT and thermodynamics. Physical Chemistry Chemical Physics, 2015, 17, 19446-19456.	2.8	50
124	Coverage Dependent Water Dissociative Adsorption on the Clean and O-Precovered Fe(111) Surfaces. Journal of Physical Chemistry C, 2015, 119, 11714-11724.	3.1	27
125	Coverage dependent adsorption and co-adsorption of CO and H <sub>2</sub> on the CdI <sub>2</sub> -antitype metallic Mo <sub>2</sub> C(001) surface. Physical Chemistry Chemical Physics, 2015, 17, 1907-1917.	2.8	17
126	Adsorption and energetics of H2O molecules and O atoms on the χ-Fe5C2 (111), (Ⱂ411) and (001) surfaces from DFT. Applied Catalysis A: General, 2014, 475, 186-194.	4.3	14

#	Article	IF	CITATIONS
127	Stable surface terminations of orthorhombic Mo2C catalysts and their CO activation mechanisms. Applied Catalysis A: General, 2014, 478, 146-156.	4.3	37
128	Hydrogen Adsorption Structures and Energetics on Iron Surfaces at High Coverage. Journal of Physical Chemistry C, 2014, 118, 4181-4188.	3.1	84
129	High Coverage CO Adsorption and Dissociation on the Orthorhombic Mo <sub>2</sub> C(100) Surface. Journal of Physical Chemistry C, 2014, 118, 3162-3171.	3.1	52
130	High Coverage CO Activation Mechanisms on Fe(100) from Computations. Journal of Physical Chemistry C, 2014, 118, 1095-1101.	3.1	54
131	High Coverage Water Aggregation and Dissociation on Fe(100): A Computational Analysis. Journal of Physical Chemistry C, 2014, 118, 26139-26154.	3.1	47
132	Structures and energies of Cu clusters on Fe and Fe <sub>3</sub> C surfaces from density functional theory computation. Physical Chemistry Chemical Physics, 2014, 16, 26997-27011.	2.8	11
133	Mild and selective hydrogenation of aromatic and aliphatic (di)nitriles with a well-defined iron pincer complex. Nature Communications, 2014, 5, 4111.	12.8	260
134	Adsorption Structures and Energies of Cun Clusters on the Fe(110) and Fe3C(001) Surfaces. Journal of Physical Chemistry C, 2014, 118, 21963-21974.	3.1	14
135	Dissociative Hydrogen Adsorption on the Hexagonal Mo <sub>2</sub> C Phase at High Coverage. Journal of Physical Chemistry C, 2014, 118, 8079-8089.	3.1	60
136	Iridium atalyzed Hydrogenation of Carboxylic Acid Esters. ChemCatChem, 2014, 6, 2810-2814.	3.7	65
137	Molybdenum carbide catalysed hydrogen production from formic acid – A density functional theory study. Journal of Power Sources, 2014, 246, 548-555.	7.8	45
138	Hydrogenation of Esters to Alcohols with a Wellâ€Defined Iron Complex. Angewandte Chemie - International Edition, 2014, 53, 8722-8726.	13.8	269
139	Copper Promotion in CO Adsorption and Dissociation on the Fe(100) Surface. Journal of Physical Chemistry C, 2014, 118, 20472-20480.	3.1	30
140	Coverage-Dependent CO Adsorption and Dissociation Mechanisms on Iron Surfaces from DFT Computations. ACS Catalysis, 2014, 4, 1991-2005.	11.2	95
141	Hydrogen generation from formic acid decomposition on Ni(211), Pd(211) and Pt(211). Journal of Molecular Catalysis A, 2013, 379, 169-177.	4.8	38
142	Density functional theory study into H2O dissociative adsorption on the Fe5C2(010) surface. Applied Catalysis A: General, 2013, 468, 370-383.	4.3	25
143	Fineâ€Tuning the Reactivity and Stability by Systematic Ligand Variations in CpCo <sup>I</sup> Complexes as Catalysts for [2+2+2] Cycloaddition Reactions. Chemistry - A European Journal, 2013, 19, 2548-2554.	3.3	52
144	Surface morphology of HÃǥg iron carbide (χ-Fe5C2) from ab initio atomistic thermodynamics. Journal of Catalysis, 2012, 294, 47-53.	6.2	90

#	Article	IF	CITATIONS
145	Formic Acid Dehydrogenation on Ni(111) and Comparison with Pd(111) and Pt(111). Journal of Physical Chemistry C, 2012, 116, 4149-4156.	3.1	115
146	Energetics of Carbon deposition on Fe(100) and Fe(110) surfaces and subsurfaces. Surface Science, 2012, 606, 733-739.	1.9	30
147	Mechanisms and Energies of Water Gas Shift Reaction on Fe-, Co-, and Ni-Promoted MoS <sub>2</sub> Catalysts. Journal of Physical Chemistry C, 2012, 116, 25368-25375.	3.1	53
148	Adsorption Equilibria of CO Coverage on β-Mo <sub>2</sub> C Surfaces. Journal of Physical Chemistry C, 2012, 116, 6340-6348.	3.1	53
149	Stability of β-Mo <sub>2</sub> C Facets from ab Initio Atomistic Thermodynamics. Journal of Physical Chemistry C, 2011, 115, 22360-22368.	3.1	108
150	Synthesis of Group 9 Metalâ€Olefin Complexes with Identical Ligand Frameworks and Comparison of their Catalytic Activity in [2+2+2] Cycloaddition and other Addition Reactions. Advanced Synthesis and Catalysis, 2011, 353, 3423-3433.	4.3	30
151	The Mechanism of Potassium Promoter: Enhancing the Stability of Active Surfaces. Angewandte Chemie - International Edition, 2011, 50, 7403-7406.	13.8	141
152	On the Role of a Cobalt Promoter in a Water-Gas-Shift Reaction on Co-MoS <sub>2</sub> . Journal of Physical Chemistry C, 2010, 114, 16669-16676.	3.1	42
153	CO2 dissociation on Ni(211). Surface Science, 2009, 603, 2991-2998.	1.9	47
154	Density functional theory study of H2 adsorption on the (100), (001) and (010) surfaces of Fe3C. Journal of Molecular Catalysis A, 2008, 292, 14-20.	4.8	20
155	CO Adsorption on Fe <sub>4</sub> C (100), (110), and (111) Surfaces in Fischerâ^'Tropsch Synthesis. Journal of Physical Chemistry C, 2008, 112, 19018-19029.	3.1	25
156	Formation of CHx Species from CO Dissociation on Double-Stepped Co(0001): Exploring Fischerâ^'Tropsch Mechanism. Journal of Physical Chemistry C, 2008, 112, 14108-14116.	3.1	71
157	Adsorption and Dissociation of CO as Well as CH <i><sub>x</sub></i> Coupling and Hydrogenation on the Clean and Oxygen Pre-covered Co(0001) Surfaces. Journal of Physical Chemistry C, 2008, 112, 3840-3848.	3.1	36
158	Kinetic aspect of CO2 reforming of CH4 on Ni(111): A density functional theory calculation. Surface Science, 2007, 601, 1271-1284.	1.9	140
159	Density functional theory study of CO adsorption on the (100), (001) and (010) surfaces of Fe3C. Journal of Molecular Catalysis A, 2007, 269, 169-178.	4.8	60
160	CO dissociation on clean and hydrogen precovered Fe(111) surfaces. Journal of Catalysis, 2007, 249, 174-184.	6.2	102
161	Formation of Carbon Species on Ni(111):  Structure and Stability. Journal of Physical Chemistry C, 2007, 111, 10894-10903.	3.1	38
162	CO2Reforming of CH4on Ni(111):Â A Density Functional Theory Calculation. Journal of Physical Chemistry B, 2006, 110, 9976-9983.	2.6	124

#	Article	IF	CITATIONS
163	Reply to "Comment on â€~Density Functional Theory Study of Triangular Molybdenum Sulfide Nanocluster and CO Adsorption on It'― Journal of Physical Chemistry B, 2006, 110, 14004-14005.	2.6	4
164	Density Function Theory Study of CO Adsorption on Fe3O4(111) Surface. Journal of Physical Chemistry B, 2006, 110, 13920-13925.	2.6	73
165	Density functional theory study into the adsorption of CO2, H and CHx (x=0–3) as well as C2H4 on α-Mo2C(0001). Surface Science, 2006, 600, 2329-2337.	1.9	54
166	Density Functional Theory Study of Triangular Molybdenum Sulfide Nanocluster and CO Adsorption on It. Journal of Physical Chemistry B, 2005, 109, 13704-13710.	2.6	33
167	Structures and Energies of Coadsorbed CO and H2on Fe5C2(001), Fe5C2(110), and Fe5C2(100). Journal of Physical Chemistry B, 2005, 109, 10922-10935.	2.6	46
168	Density Functional Theory Study of Hydrogen Adsorption on Fe5C2(001), Fe5C2(110), and Fe5C2(100). Journal of Physical Chemistry B, 2005, 109, 833-844.	2.6	43
169	Density functional theory study of CO adsorption on the Fe(111) surface. Chemical Physics Letters, 2004, 400, 35-41.	2.6	33
170	Density Functional Theory Study of CO Adsorption on Fe5C2(001), -(100), and -(110) Surfaces. Journal of Physical Chemistry B, 2004, 108, 9094-9104.	2.6	62
171	Acetylene Hydroformylation with HCo(CO)3 as Catalyst. A Density Functional Study. Organometallics, 2004, 23, 765-773.	2.3	14
172	A new strategy for the efficient synthesis of 2-methylfuran and Î <sup>3</sup> -butyrolactone. New Journal of Chemistry, 2003, 27, 208-210.	2.8	62
173	Accurate Calculations of Bond Dissociation Enthalpies with Density Functional Methods. Journal of Physical Chemistry A, 2003, 107, 9991-9996.	2.5	107
174	The Structure and Possible Catalytic Sites of Mo3S9as a Model of Amorphous Molybdenum Trisulfide:Â A Computational Study. Journal of the American Chemical Society, 2001, 123, 7334-7339.	13.7	39
175	Nucleus-Independent Chemical Shifts:  A Simple and Efficient Aromaticity Probe. Journal of the American Chemical Society, 1996, 118, 6317-6318.	13.7	5,447
176	Baseâ€Mediated Remote Deuteration of <i>N</i> â€Heteroarenes – Broad Scope and Mechanism. European Journal of Organic Chemistry, 0, , .	2.4	4